5

Sensitivity Operators on L_2

This chapter studies the computation of L_2-induced norms of sampled-data sensitivity operators. The L_2-induced norm is the operator norm when inputs and outputs belong to the space of square-integrable signals L_2, and it is closely related to important control problems. Indeed, for LTI systems, the L_2-induced norm of a system's operator is the H_∞-norm of its transfer matrix, which represents an extremely useful measure in many applications of modern control theory [e.g., Francis, 1991].

Concepts and methods associated with LTI H_∞ control bear no immediate equivalent for sampled-data systems, since in this case the operators are time-varying and no transfer functions are associated with them. In view of this, considerable research during the last years has focused on the study of L_2-norms and H_∞ related problems for sampled-data systems.

Early works considering L_2-norms for hybrid systems studied restricted classes of sampled-data systems Thompson et al. [1983, 1986], Chen and Francis [1990], Leung et al. [1991]. Conic sectors were applied by Thompson et al. [1983] and Thompson et al. [1986] to obtain upper bounds for the L_2-norm of cascade connections involving a sampler and a ZOH. Exact expressions for these open-loop systems appeared later on in Chen and Francis [1990]. A formula for the L_2-norm of hybrid operators in a general feedback configuration was derived by Leung et al. [1991] for the case of band-limited signals.

More recent works introduced the use of *lifting* techniques for the H_∞ analysis and synthesis of sampled-data systems Bamieh and Pearson [1992], Toivonen [1992], Yamamoto [1990, 1993]. As mentioned in Chapter 1, the lifting technique transforms the sampled-data system into a discrete time-invariant equivalent system acting over infinite-dimensional signals. Time-invariance comes as a consequence of periodicity, but in contrast to the classical pure discrete approach, intersample behavior is built in the model, which is reflected in the infinite dimensionality of the transformed signals. Sampled-data H_∞-norm computation and optimization Bamieh and Pearson [1992], Toivonen [1992], Yamamoto [1993], robust stabilization to LTI perturbations Dullerud and Glover [1993], and tracking Yamamoto [1994] are some recent results obtained via lifting.

Other time-domain approaches include the formulation of an associated Hamiltonian descriptor system Kabamba and Hara [1993], and the solution of continuous and discrete Riccati equations derived using the theory of linear systems with

jumps Sivashankar and Khargonekar [1994], Sun et al. [1993], Tadmor [1991].

An interesting and novel application derived from the computation of L_2-norms is the extension of the LTI concept of frequency-gain to sampled-data systems Araki and Ito [1993], Araki et al. [1993], Yamamoto and Khargonekar [1996], Hagiwara et al. [1995], Yamamoto and Araki [1994]. The so-called frequency-gain of a sampled-data system is equivalent to the magnitude of a Bode plot of certain discrete transfer function associated with the hybrid system. In Yamamoto and Khargonekar [1996] lifting techniques were used to compute the frequency-gain of a sampled-data system. In Hagiwara et al. [1995] the same issue was addressed using a frequency-domain framework that uses the notion of FR-operators Araki and Ito [1993], Araki et al. [1993].

Our approach in this chapter evolves from the frequency-domain formulation introduced in Chapter 4. In §5.1 we expound a *frequency-domain lifting* framework, which further exposes the harmonic structure of the sampled-data system, yielding a compact description of the operators that govern its behavior. This framework is equivalent to that of FR-operators introduced by Araki and Ito [1993] and Araki et al. [1993]. Yet, our formulation builds up on spaces of Fourier transforms of the original signals, while the FR-operators are defined on special spaces of time-domain signals called SD-sinusoids. The advantages of both methods over time-domain alternatives are similar, and arise from the simplicity of the frequency-domain description.

In §5.2 we exploit the benefits of the frequency-domain lifting to compute the L_2-induced norms and frequency-gains of sampled-data sensitivity and complementary sensitivity operators. Note that the complementary sensitivity operator is a finite-rank operator — and therefore compact — which implies that its norm can be computed relatively easily. On the other hand, the sensitivity operator is non-compact, which imposes a greater difficulty in the computation of its norm Yamamoto and Khargonekar [1996]. We show that either norm and the frequency-gains can be computed in a straightforward way from finite dimensional discrete transfer functions. The expressions derived are easily implemented in numerically reliable algorithms, as we show in §5.2.2.

5.1 A Frequency-domain Lifting

Many important concepts and methods for LTI systems have no immediate extension to sampled-data systems for the simple fact that sampled-data systems are time-varying. Nevertheless, they belong to a particular class of time-varying systems that have a lot of structure, namely, they can be represented by periodic operators. Most of recent advances in sampled-data control theory have been based on mathematical frameworks that profit from this periodic characteristic. An example of this is the time-domain lifting technique of Bamieh and Pearson [1992] and Yamamoto 1990, 1994. By lifting, a signal valued in a finite dimensional space is bijectively mapped into a signal valued in infinite dimensional spaces. The great attractiveness of the transformation lies on the fact that in the new spaces the operators are represented as LTI operators, which allow a simpler

treatment of many important problems.

In this section we describe a similar mathematical formalism that we call the *frequency-domain* lifting[1]. The lifting of Bamieh and Pearson [1992] and Yamamoto [1994] is done over signals in the time-domain, which leads to state-space representations of the sampled-data system. The main difference in our approach is that we lift signals directly in frequency-domain, which — as we shall see in the remaining sections of this chapter — may allow a simpler and more intuitive treatment[2] of problems that are naturally formulated in input-output scenarios.

Consider a signal y in the space $L_2(0,\infty)$. Then, its Fourier transform $Y(j\omega)$ is known to belong to $L_2(-\infty,\infty)$. Introduce the following sequence of functions constructed from $Y(j\omega)$,

$$Y_k(j\omega) = Y(j(\omega + k\omega_s)), \tag{5.1}$$

for ω in the Nyquist range Ω_N and k integer. We arrange this sequence in an infinite vector, and we denote it by

$$\mathbf{y}(\omega) \triangleq \begin{bmatrix} \vdots \\ Y_1(j\omega) \\ Y_0(j\omega) \\ Y_{-1}(j\omega) \\ \vdots \end{bmatrix}. \tag{5.2}$$

We say that the infinite vector $\mathbf{y}(\omega)$ is the — frequency-domain — *lifting* of the signal $Y(j\omega)$. Figure 5.1 illustrates the action of the lifting operation, which chops up the function $Y(j\omega)$ defined on $(-\infty,\infty)$ into a sequence of functions $Y_k(j\omega)$, $k = 0, \pm1, \pm2, \ldots$ defined on Ω_N.

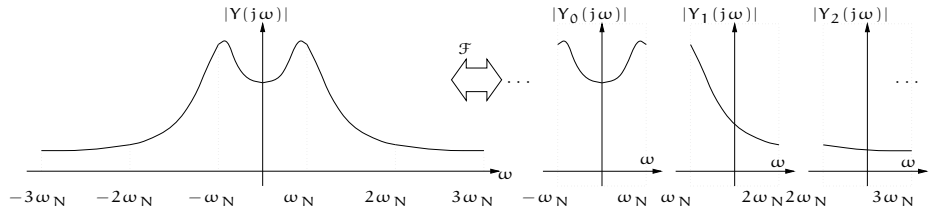

Figure 5.1: Action of the frequency-domain lifting operation.

Thus, $\mathbf{y}(\omega)$ can be seen as a function defined a.e.[3] over Ω_N taking values in ℓ_2. Moreover, the space of such functions is a Hilbert space under the norm

$$\|\mathbf{y}\| \triangleq \left(\int_{\Omega_N} \|\mathbf{y}(\omega)\|_{\ell_2}^2 \, d\omega \right)^{1/2}, \tag{5.3}$$

[1]The concept of frequency-domain lifting is not new; it was developed in the signal processing literature for linear discrete-time periodic systems [e.g., Shenoy et al., 1994].

[2]Simpler and more intuitive in the sense explained in Chapter 1, §1.2 (i).

[3]With respect to the standard Lebesgue measure.

and inner product

$$\langle \mathbf{y}, \mathbf{x} \rangle \triangleq \int_{\Omega_N} \langle \mathbf{y}(\omega), \mathbf{x}(\omega) \rangle_{\ell_2} \, \mathrm{d}\omega \; . \tag{5.4}$$

We denote this space by $L_2(\Omega_N; \ell_2)$ [cf. Balakrishnan, 1981]. Since the signals in $L_2(\Omega_N; \ell_2)$ are basically rearrangements of signals in $L_2(-\infty, \infty)$, it is not difficult to see that both spaces are isomorphic with preservation of norm, as the following lemma asserts.

Lemma 5.1.1
The space $L_2(\Omega_N; \ell_2)$ *is isometrically isomorphic to* $L_2(-\infty, \infty)$.

Proof: See Appendix A, §A.4. □

Lemma 5.1.1 tells us that there is a bijective relation between elements in $L_2(-\infty, \infty)$ and elements in $L_2(\Omega_N; \ell_2)$, and moreover, they have the same measure, i.e.,

$$\|\mathbf{y}\|_{L_2(\Omega_N; \ell_2)} = \|Y\|_{L_2(-\infty, \infty)}.$$

We formalize this relationship by defining the *frequency-domain lifting operator*, $\mathcal{F}$, mapping

$$\begin{array}{rcl} \mathcal{F} : L_2(-\infty, \infty) & \to & L_2(\Omega_N; \ell_2) \\ Y(j\omega) & \mapsto & \mathbf{y}(\omega) \; . \end{array}$$

Evidently from Lemma 5.1.1, $\mathcal{F}$ is invertible, and moreover, $\|\mathcal{F}\| = 1 = \|\mathcal{F}^{-1}\|$. In particular, if $\mathcal{M}$ is a bounded linear operator from $L_2(-\infty, \infty)$ to $L_2(-\infty, \infty)$, then the lifted operator $\mathfrak{M} = \mathcal{F}\mathcal{M}\mathcal{F}^{-1}$ is a bounded linear operator from $L_2(\Omega_N; \ell_2)$ to $L_2(\Omega_N; \ell_2)$ with the same operator norm. A key observation at this point is that it will be in general easier and numerically more tractable to compute $\|\mathfrak{M}\|$ rather than $\|\mathcal{M}\|$.

The representation of sampled-data operators by their liftings also reveals structure with interesting similarities to ordinary LTI operators and their corresponding transfer matrices. Indeed, it turns out that the lifted operator $\mathfrak{M}$ is a *multiplication operator* in ℓ_2 sense, so it has an associated representation as an infinite-dimensional "transfer matrix". In other words, we can write $(\mathfrak{M}\mathbf{y})(\omega) = \mathbf{M}_\omega \mathbf{y}(\omega)$, where $\mathbf{M}_\omega$ is a bounded linear operator in ℓ_2 at (almost) every fixed ω in Ω_N. An important consequence of this fact is that the L_2-induced norm of the operator can be computed as [cf. Yamamoto and Khargonekar, 1996]

$$\|\mathcal{M}\| = \sup_{\omega \in \Omega_N} \|\mathbf{M}_\omega\|_{\ell_2}, \tag{5.5}$$

where $\|\mathbf{M}_\omega\|_{\ell_2}$ denotes the induced ℓ_2-norm of the operator M_ω. Notice the similarity of (5.5) to the familiar expression of the L_2-induced norm of an operator in a LTI system, i.e., the H_∞-norm of its associated transfer matrix.

In particular, we shall be concerned with *compact* and *approximable* operators on these spaces, so we finish the section with a brief discussion of these concepts. This follows Willis [1994].

Recall that a set K in a metric space is *compact* if each sequence in K has a convergent subsequence. Equivalently, for any collection of open sets $\{V_k\}$ that covers K, then K is compact if and only if $\{V_k\}$ has a finite subcollection that covers K. To say that a set is compact is to say that it is "small" in some sense. The Heine-Borel Theorem [e.g., Rudin, 1987] asserts that a set in a finite-dimensional space is compact if and only if it is closed and bounded.

Definition 5.1.1 (Compact Operator)
Let X and Y be metric spaces, and let B_X denote the unit ball in X. Then the operator $T : X \to Y$ is said to be compact if the closure of $T(B_X)$ is a compact set. ◇

Compact operators are very close to finite-rank operators, i.e., operators whose range is finite-dimensional. Since $T(B_X)$ is bounded if T is a bounded operator, it follows from the Heine-Borel Theorem that each finite-rank operator is compact. In a sense, a "converse" of this is also true in the spaces we are interested in. Namely, a compact operator on these spaces is *approximable* by sequences of finite-rank operators; i.e., if $\{E_n\}$ is a sequence of finite-rank operators, then $\lim_{n\to\infty} \|E_n - T\| = 0$, where $\|\cdot\|$ denotes the induced operator norm.

5.2 L_2-induced Norms and Frequency-gains

5.2.1 Sensitivity Operators

We study the sensitivity and complementary sensitivity operators for the sampled-data system of Figure 2.4. As for LTI systems, we define these operators as the mappings relating output disturbance d and noise n to the output y, and denote them respectively by

$$\begin{array}{rcl} \mathcal{S} : L_2 & \to & L_2 \\ \mathcal{S}d & \mapsto & y \end{array} \quad \text{and} \quad \begin{array}{rcl} \mathcal{T} : L_2 & \to & L_2 \\ \mathcal{T}n & \mapsto & y. \end{array}$$

Under the assumptions of closed-loop L_2-stability, $\mathcal{S}$ and $\mathcal{T}$ are bounded operators on L_2.

The actions of the sensitivity and complementary sensitivity operators are respectively defined in frequency-domain by the steady-state responses (4.1) and (4.2) introduced in Chapter 4, §4.1. From the definition of frequency-domain lifting in §5.1, it is straightforward to alternatively write (4.1) and (4.2) evaluated at $s = j\omega$ in a very compact form as

$$\mathbf{y} = \mathbf{S}_\omega \mathbf{d} \qquad \text{and} \qquad \mathbf{y} = -\mathbf{T}_\omega \mathbf{n}\,, \tag{5.6}$$

where $\mathbf{T}_\omega$ and $\mathbf{S}_\omega$ are the following infinite-dimensional transfer matrices defined on Ω_N

$$\mathbf{T}_\omega = \begin{bmatrix} \ddots & \vdots & \vdots & \\ \cdots & G_k F_k & G_k F_{k-1} & \cdots \\ \cdots & G_{k-1} F_k & G_{k-1} F_{k-1} & \cdots \\ & \vdots & \vdots & \ddots \end{bmatrix}, \tag{5.7}$$

$$\mathbf{S}_\omega = \begin{bmatrix} \ddots & \vdots & \vdots & \\ \cdots & 1 - G_k F_k & -G_k F_{k-1} & \cdots \\ \cdots & -G_{k-1} F_k & 1 - G_{k-1} F_{k-1} & \cdots \\ & \vdots & \vdots & \ddots \end{bmatrix}, \tag{5.8}$$

where, to ease notation, we have omitted the explicit dependence of the variable $j\omega$ in the entries of the matrices. Keep also in mind the notation $F_k(j\omega)$ representing $F(j(\omega + k\omega_s))$, which will be profusely used in the sequel. Here $F(j\omega)$ is the transfer matrix of the anti-aliasing filter, and the function $G(j\omega)$ denotes the product

$$G(j\omega) \triangleq \frac{1}{T} P(j\omega) H(j\omega) S_d(e^{j\omega T}) C_d(e^{j\omega T}). \tag{5.9}$$

Associated with $F(j\omega)$ and $G(j\omega)$ we define the following discretized transfer matrices that will be required to formulate our results,

$$G_d(e^{j\omega T}) \triangleq \sum_{k=-\infty}^{\infty} G_k^*(j\omega) G_k(j\omega), \tag{5.10}$$

and

$$F_d(e^{j\omega T}) \triangleq \sum_{k=-\infty}^{\infty} F_k(j\omega) F_k^*(j\omega), \tag{5.11}$$

where F^* denotes the conjugated transpose of F. Note that if y, n, and d are valued in $\mathbb{R}^m$, then $G_d(e^{j\omega T})$ and $F_d(e^{j\omega T})$ are $m \times m$ discrete transfer matrices.

Operators $\mathbf{S}_\omega$ and $\mathbf{T}_\omega$ are infinite-dimensional transfer matrix representations of the hybrid sensitivity and complementary sensitivity operators $\mathcal{S}$ and $\mathcal{T}$, and verify the complementarity relation $\mathbf{S}_\omega + \mathbf{T}_\omega = \mathbf{I}$ [cf. Araki and Ito, 1993, Araki et al., 1993, Yamamoto and Araki, 1994]. From (5.5) their induced norms are given by

$$\|\mathcal{T}\| = \sup_{\omega \in \Omega_N} \|\mathbf{T}_\omega\|_{\ell_2} \quad \text{and} \quad \|\mathcal{S}\| = \sup_{\omega \in \Omega_N} \|\mathbf{S}_\omega\|_{\ell_2}, \tag{5.12}$$

and so, they can be evaluated by computing the functions $\|\mathbf{T}_\omega\|_{\ell_2}$ and $\|\mathbf{S}_\omega\|_{\ell_2}$ — the so-called *frequency-gains* of the hybrid operators [e.g., Hagiwara et al., 1995] — and then searching for suprema over the finite interval Ω_N.

An important fact about the complementary sensitivity operator $\mathcal{T}$ is that it has finite rank (and therefore is compact, as discussed in §5.1). We show this in the following lemma.

Lemma 5.2.1
If the inputs to the system in Figure 2.4 are valued in $\mathbb{R}^m$, then $\mathcal{T}$ has at most rank m.

Proof: Partition $F(j\omega)$ by rows, and $G(j\omega)$ by columns, i.e.,

$$F(j\omega) = \begin{bmatrix} f_1(j\omega) \\ f_2(j\omega) \\ \vdots \\ f_m(j\omega) \end{bmatrix}, \quad \text{and} \quad G(j\omega) = \begin{bmatrix} g_1(j\omega) & g_2(j\omega) & \cdots & g_m(j\omega) \end{bmatrix}.$$

Introduce the liftings for $F^*(j\omega)$ and $G(j\omega)$,

$$\mathbf{f}(\omega) \triangleq \begin{bmatrix} \vdots \\ F_1^*(j\omega) \\ F_0^*(j\omega) \\ F_{-1}^*(j\omega) \\ \vdots \end{bmatrix}, \quad \text{and} \quad \mathbf{g}(\omega) \triangleq \begin{bmatrix} \vdots \\ G_1(j\omega) \\ G_0(j\omega) \\ G_{-1}(j\omega) \\ \vdots \end{bmatrix}. \tag{5.13}$$

Using the partitions above, we can alternatively write

$$\mathbf{f}(\omega) = \begin{bmatrix} \mathbf{f}_1(\omega) & \mathbf{f}_2(\omega) & \dots & \mathbf{f}_m(\omega) \end{bmatrix},$$

and

$$\mathbf{g}(\omega) = \begin{bmatrix} \mathbf{g}_1(\omega) & \mathbf{g}_2(\omega) & \dots & \mathbf{g}_m(\omega) \end{bmatrix},$$

where each column $\mathbf{f}_i = \mathcal{F}f_i^*$ in $\mathbf{f}$, and $\mathbf{g}_i = \mathcal{F}g_i$ in $\mathbf{g}$ is certainly a vector in $L_2(\Omega_N; \ell_2)$, since F and G are both stable and strictly proper from our assumptions in Chapter 2. Using this notation, the action of $\mathbf{T}_\omega$ can be alternatively written as

$$\mathbf{T}_\omega \mathbf{n} = \sum_{i=1}^{m} \mathbf{g}_i \langle \mathbf{n}, \mathbf{f}_i \rangle_{\ell_2}, \tag{5.14}$$

where, $\langle \mathbf{n}, \mathbf{f}_i \rangle_{\ell_2}$ is a scalar-valued function defined a.e. on Ω_N[4]. Equation (5.14) shows that $\mathbf{T}_\omega$ is the sum of m rank-one operators on $L_2(\Omega_N; \ell_2)$. Hence it has at most rank m, and so does $\mathcal{T}$. □

The fact that $\mathcal{T}$ is compact — and so approximable — suggests a way of numerically computing the norm of $\mathcal{T}$ by truncating $\mathbf{T}_\omega$ between harmonics $-n$ and n, say, and evaluating the maximum singular value of the finite dimensional transfer matrix so obtained Araki et al. [1993]. The convergence of this sequence of computations could be slow, though, since in general $G(j\omega)$ and $F(j\omega)$ decay as $1/\omega^p$, where p is some integer depending on the relative degrees of the transfer matrices involved.

Actually, since $\mathcal{T}$ is of finite-rank, more efficient ways of numerically evaluating the induced norm of $\mathbf{T}_\omega$ are possible and already available. Using frequency-domain techniques similar to ours, Hagiwara et al. [1995] have shown that the computation of the frequency-gain of a compact operator can be obtained as the magnitude of an associated discrete-time transfer matrix. For the case of ZOH, they show how to implement their procedures in a numerically reliable fashion.

The following theorem is analogous to the result of Hagiwara et al. [1995] for the case of the hybrid complementary sensitivity operator $\mathcal{T}$. The pattern of our proof is quite different though, and importantly, we shall use the same pattern for the more difficult case of the hybrid sensitivity operator, which is non-compact. Our results extend to the case of GSHF, and are also implementable in a numerically reliable way, as we shall see in Subsection 5.2.2.

[4]Often, we shall drop the dependence of the independent variable when convenient; meaning will always be clear from context.

We denote by $\lambda_{max}[M]$ the maximum eigenvalue of a square matrix M. Then we have the following result.

Theorem 5.2.2 (L_2-induced Norm of the Complementary Sensitivity Operator) *If the hybrid system of Figure 2.4 is L_2-input-output stable, then*

$$\|\mathcal{T}\|^2 = \sup_{\omega\in\Omega_N} \lambda_{max}\left[G_d(e^{j\omega T})F_d(e^{j\omega T})\right] . \tag{5.15}$$

Proof: Using (5.13) write $\mathbf{T}_\omega$ as a dyadic product

$$\mathbf{T}_\omega = \mathbf{g}(\omega)\mathbf{f}(\omega)^*,$$

where $\mathbf{f}^*$ denotes the conjugate transpose of $\mathbf{f}$ (i.e., $\mathbf{f}^*$ is composed of "row" vectors of $L_2(\Omega_N, \ell_2)$). From (5.12) we have that $\|\mathcal{T}\| = \sup_{\omega\in\Omega_N} \|\mathbf{T}_\omega\|_{\ell_2}$. Fix ω in Ω_N, and decompose ℓ_2 into

$$\ell_2 = P_F \oplus P_F^\perp,$$

where P_F is the subspace of ℓ_2 spanned by the range of $\mathbf{f}$, and $P_F^\perp$ its orthogonal complement. Hence, if $\mathbf{v}$ is a vector in $P_F^\perp$ then $\mathbf{T}_\omega\mathbf{v} = 0$. So,

$$\begin{aligned}\|\mathbf{T}_\omega\|_{\ell_2} &= \sup_{\substack{v\in\ell_2\\ v\neq 0}} \frac{\|\mathbf{T}_\omega\mathbf{v}\|_{\ell_2}}{\|\mathbf{v}\|_{\ell_2}} \\ &= \sup_{\substack{v\in P_F\\ v\neq 0}} \frac{\|\mathbf{T}_\omega\mathbf{v}\|_{\ell_2}}{\|\mathbf{v}\|_{\ell_2}}.\end{aligned}$$

Vectors of ℓ_2 in P_F can be finitely parameterized as

$$\mathbf{v} = \mathbf{f}\alpha,$$

where α belongs to $\mathbb{C}^m$, with m the number of inputs of F. Thus, we have

$$\begin{aligned}\|\mathbf{T}_\omega\|_{\ell_2}^2 &= \sup_{\substack{\alpha\\ \mathbf{f}\alpha\neq 0}} \frac{\alpha^*\mathbf{f}^*\mathbf{f}\mathbf{g}^*\mathbf{g}\mathbf{f}^*\mathbf{f}\alpha}{\alpha^*\mathbf{f}^*\mathbf{f}\alpha} \\ &= \lambda_{max}\left[(\mathbf{f}^*\mathbf{f})^{1/2}(\mathbf{g}^*\mathbf{g})(\mathbf{f}^*\mathbf{f})^{1/2}\right]. \end{aligned}\tag{5.16}$$

Notice that both $(\mathbf{g}^*\mathbf{g})$ and $(\mathbf{f}^*\mathbf{f})$ are finite $m \times m$ matrices, and particularly, $\mathbf{f}^*\mathbf{f}$ is non-singular since F was assumed full column rank.

Since eigenvalues are invariant under similarity transformations, (5.16) yields

$$\|\mathbf{T}_\omega\|_{\ell_2}^2 = \lambda_{max}\left[(\mathbf{g}^*\mathbf{g})(\mathbf{f}^*\mathbf{f})\right].$$

The proof is finished by noting that

$$(\mathbf{g}^*\mathbf{g})(\omega) = G_d(e^{j\omega T})$$

and

$$(\mathbf{f}^*\mathbf{f})(\omega) = F_d(e^{j\omega T})$$

are the discrete transfer matrices defined in (5.10) and (5.11). □

The case of $\mathcal{S}$ has to be considered more carefully, since this is a non-compact operator, and as such, it may not be in principle approximable by sequences of finite-rank operators (which means that the norms of progressive truncations of $\mathbf{S}_\omega$ would not necessarily converge to the norm of the operator). Frequency-gains of possibly non-compact sampled-data operators have been discussed in Yamamoto and Khargonekar [1996]. Their method computes the frequency-gain γ_ω at the frequency ω by searching for the maximum value γ such that a γ-dependent generalized eigenvalue problem has an eigenvalue $e^{j\omega T}$. Yet, the procedure seems in general very hard to be implemented numerically in a reliable fashion Hagiwara et al. [1995].

The following theorem gives an expression for the frequency-gain and L_2-induced norm of the hybrid sensitivity operator $\mathcal{S}$. Our result relies on the fact that $\mathcal{S}$ verifies the complementarity relation

$$\mathcal{S} = \mathcal{I} - \mathcal{T},$$

and since $\mathcal{T}$ is of finite rank, it is also possible to reduce the computation of the frequency-gain of $\mathcal{S}$ to a finite-dimensional eigenvalue problem. As for Theorem 5.2.2, these results admit a simple and reliable numerical implementation.

Theorem 5.2.3 (L_2-induced Norm of the Sensitivity Operator)
If the hybrid system of Figure 2.4 is L_2-input-output stable, then

$$\|\mathcal{S}\|^2 = 1 + \sup_{\omega\in\Omega_N} \lambda_{\max} \begin{bmatrix} F_d(e^{j\omega T})\, G_d(e^{j\omega T}) - T_d(e^{j\omega T}) & -F_d(e^{j\omega T}) \\ T_d(e^{-j\omega T})\, G_d(e^{j\omega T}) - G_d(e^{j\omega T}) & -T_d(e^{-j\omega T}) \end{bmatrix}. \quad (5.17)$$

Proof: The same idea for the proof of Theorem 5.2.2 works here. Again, for a fixed ω in Ω_N, decompose ℓ_2 into

$$\ell_2 = P_{(F,G)} \oplus P_{(F,G)}^{\perp},$$

where $P_{(F,G)}$ denotes the subspace spanned by both $\mathbf{f}$ and $\mathbf{g}$, and $P_{(F,G)}^{\perp}$ its orthogonal complement. Since $\mathbf{S}_\omega$ is block diagonal in these spaces,

$$\begin{aligned} \|\mathbf{S}_\omega\|_{\ell_2} &= \max \left\{ \sup_{\substack{v\in P_{(F,G)} \\ v\neq 0}} \frac{\|\mathbf{S}_\omega \mathbf{v}\|_{\ell_2}}{\|\mathbf{v}\|_{\ell_2}} \;,\; \sup_{\substack{v\in P_{(F,G)^\perp} \\ v\neq 0}} \frac{\|\mathbf{S}_\omega \mathbf{v}\|_{\ell_2}}{\|\mathbf{v}\|_{\ell_2}} \right\} \\ &= \max \left\{ \sup_{\substack{v\in P_{(F,G)} \\ v\neq 0}} \frac{\|\mathbf{S}_\omega \mathbf{v}\|_{\ell_2}}{\|\mathbf{v}\|_{\ell_2}} \;,\; 1 \right\}. \end{aligned} \quad (5.18)$$

Now, any vector $\mathbf{v}$ in $P_{(F,G)}$ can be finitely parameterized as

$$\begin{aligned} \mathbf{v} &= \mathbf{f}\alpha + \mathbf{g}\beta \\ &= [\mathbf{f}, \mathbf{g}]\, \gamma, \end{aligned} \quad (5.19)$$

with γ in C^{2m}. Denote $\mathbf{h} \triangleq [\mathbf{f}, \mathbf{g}]$, and $M \triangleq \mathbf{h}^*\mathbf{h}$. Notice that M is a finite-dimensional Hermitian matrix and, moreover, since for any vector η in C^{2m} we have that $\eta^* M \eta = \eta^* h^* h \eta = \|h\eta\|_2$, M is also non-negative definite, i.e., $M \geq 0$. Using the notation introduced in (5.10) and (5.11), and the definition of the discrete output complementary sensitivity function (2.11) (i.e., notice that $T_d = \mathbf{f}^*\mathbf{g}$), we can write M as

$$M = \begin{bmatrix} F_d & T_d \\ T_d^* & G_d \end{bmatrix}.$$

Introduce also the matrix N,

$$N \triangleq \begin{bmatrix} G_d & -I \\ -I & 0 \end{bmatrix}.$$

It then follows that $\mathbf{h}^*(\mathbf{I} - \mathbf{f}\mathbf{g}^*)(\mathbf{I} - \mathbf{g}\mathbf{f}^*)\mathbf{h} = (I + MN)M$, and hence we obtain from (5.19) that

$$\begin{aligned} \sup_{\substack{v \in P_{(F,G)} \\ v \neq 0}} \frac{\|\mathbf{S}_\omega \mathbf{v}\|_{\ell_2}^2}{\|\mathbf{v}\|_{\ell_2}^2} &= \sup_{\gamma \in \mathbb{C}^{2m}} \frac{\gamma^* M \gamma + \gamma^* M N M \gamma}{\gamma^* M \gamma} \\ &= 1 + \lambda_{max}\left[M^{1/2} N M^{1/2}\right] \qquad (5.20) \\ &= 1 + \lambda_{max}\left[MN\right]. \qquad (5.21) \end{aligned}$$

Since in (5.21) the product MN is

$$MN = \begin{bmatrix} F_d G_d - T_d & -F_d \\ T_d^* G_d - G_d & -T_d^* \end{bmatrix},$$

from (5.18) and (5.21) we see that it remains to show that $\lambda_{max}[MN]$ is nonnegative to complete the proof. This follows easily from the fact that $M \geq 0$. Indeed, if M is positive definite, i.e., $M > 0$, then

$$\delta = \begin{bmatrix} F_d & T_d \\ T_d^* & G_d \end{bmatrix}^{-1/2} \begin{bmatrix} I \\ 0 \end{bmatrix},$$

gives $\delta^* M^{1/2} N M^{1/2} \delta = G_d \geq 0$. Thus λ_{max} in (5.20) is nonnegative. If otherwise M is not positive definite it is then necessarily singular, and therefore 0 must be in the spectrum of $M^{1/2} N M^{1/2}$, which then shows that $\lambda_{max}[MN] \geq 0$. The proof is now complete. □

Remark 5.2.1 (L_2-norms and Hybrid Sensitivity Functions) As anticipated at the end of Chapter 4, the L_2-induced norm of these operators may be linked to certain measure of the hybrid sensitivity functions S^0, T^0, and T^k. In fact, this connection establishes that large harmonics will necessarily imply a large norm of the operator on L_2, as we shall see next. We define first the *hybrid* (k, m)*-harmonic response*

$$T^{k,m} \triangleq G_k F_m.$$

Notice that $T^{k,m}$ for $k, m = \pm 1, \pm 2, \ldots$ appear as the off-diagonal entries of the infinite-dimensional transfer matrices $\mathbf{T}_\omega$ and $\mathbf{S}_\omega$ in (5.7) and (5.8). In particular, $T^{k,0} = T^k$ and $T^{0,0} = T^0$, the harmonic and fundamental complementary sensitivity responses of Chapter 4. We require the following preliminary lemma.

Lemma 5.2.4
Let $A, B_1, B_2, \ldots, B_k, \ldots$ be square hermitian positive-definite matrices. Then

$$\lambda_{max}\left[\sum_k B_k A\right] \geq \max_k \lambda_{max}\left[B_k A\right].$$

Proof:

$$\begin{aligned}\lambda_{max}\left[\sum_k B_k A\right] &= \lambda_{max}\left[\sum_k [A^{\frac{1}{2}} B_k A^{\frac{1}{2}}]\right] \\ &= \max_{\nu, \|\nu\|=1} \sum_k [\nu^* A^{\frac{1}{2}} B_k A^{\frac{1}{2}} \nu] \\ &\geq \max_k \max_{\nu, \|\nu\|=1} \nu^* A^{1/2} B_k A^{1/2} \nu \\ &= \max_k \lambda_{max}\left[B_k A\right]\end{aligned}$$

□

Now we have the following result.

Proposition 5.2.5
Assume the conditions of Lemma 2.2.2 are satisfied. Then

$$\|\mathcal{T}\| \geq \max_{k,m} \|T_{k,m}\|_\infty$$

Proof: From Theorem 5.2.2,

$$\|\mathcal{T}\|^2 = \frac{1}{T^2} \sup_{\omega \in \Omega_N} \lambda_{max}\left[\left(\sum_k G_k^* G_k\right)\left(\sum_m F_m F_m^*\right)\right].$$

Use Lemma 5.2.4 with $A = (\sum_k G_k^* G_k)$, and $B_m = F_m F_m^*$ to get

$$\|\mathcal{T}\|^2 \geq \frac{1}{T^2} \sup_{\omega \in \Omega_N} \max_m \lambda_{max}\left[\sum_k G_k^* G_k F_m F_m^*\right],$$

and once more with $A = F_m F_m^*$, and $B_k = G_k^* G_k$. This yields

$$\begin{aligned}\|\mathcal{T}\|^2 &\geq \frac{1}{T^2} \sup_{\omega \in \Omega_N} \max_{k,m} \lambda_{max}\left[G_k^* G_k F_m F_m^*\right] \\ &= \max_{k,m} \sup_{\omega \in \Omega_N} \|\frac{1}{T} G_k F_m\|_2^2 \\ &= \max_{k,m} \|T_{k,m}\|_\infty^2.\end{aligned}$$

□

This result establishes that a peak in any of the harmonics will increase the L_2-induced norm of $\mathcal{T}$, reducing the system's stability robustness properties against T-periodic perturbations Sivashankar and Khargonekar [1993]. ◇

In the particular case of SISO systems, we can derive simpler formulas from Theorems 5.2.2 and 5.2.3. The operator $\mathcal{T}$ is then of rank one, and so the computation of its norm and the norm of $\mathcal{S}$ reduces to a single-eigenvalue problem.

Corollary 5.2.6
If the hybrid system of Figure 2.4 is SISO, then

$$\|\mathcal{T}\| = \sup_{\omega\in\Omega_N} \Phi_d(e^{j\omega T})|T_d(e^{j\omega T})|, \tag{5.22}$$

and

$$\|\mathcal{S}\| = \sup_{\omega\in\Omega_N} \frac{1}{2}\left(\sqrt{(\Phi_d^2(e^{j\omega T})-1)|T_d(e^{j\omega T})|^2 + (|S_d(e^{j\omega T})|+1)^2}\right.$$
$$+ \quad \left.\sqrt{(\Phi_d^2(e^{j\omega T})-1)|T_d(e^{j\omega T})|^2 + (|S_d(e^{j\omega T})|-1)^2}\right), \tag{5.23}$$

where

$$\Phi_d^2(e^{j\omega T}) = \frac{F_d(e^{j\omega T})\, G_d(e^{j\omega T})}{|T_d(e^{j\omega T})|^2}. \tag{5.24}$$

Proof: The proof of (5.22) follows immediately from Theorem 5.2.2. Formula (5.23) is obtained by computing λ_{max} in (5.17) and after some algebraic manipulation. □

The function Φ_d may be given some interesting interpretations that we consider in the following remarks.

Remark 5.2.2 (Φ_d as a Measure of Intersample Activity) The function Φ_d may be given an interpretation as a "fidelity function", that is, a measure of the amount of intersample behavior in the sampled-data system. Indeed, note that Φ_d is always greater than or equal to 1, since by Cauchy-Schwarz

$$\begin{aligned}|(FPH)_d(e^{j\omega T})|^2 &= \left|\frac{1}{T}\sum_{k=-\infty}^{\infty} F_k(j\omega)P_k(j\omega)H_k(j\omega)\right|^2 \\ &\leq \left(\sum_{k=-\infty}^{\infty}|F_k(j\omega)|^2\right)\left(\frac{1}{T^2}\sum_{k=-\infty}^{\infty}|P_k(j\omega)H_k(j\omega)|^2\right).\end{aligned}$$

Thus, from (5.22) we can see that

$$\|\mathcal{T}\| \leq \|\Phi_d\|_\infty \|T_d\|_\infty,$$

so $\|\Phi_d\|_\infty$ is an upper bound of the quotient between the L_2-induced norms considering full-time information, and sampled behavior respectively.

Also notice that since $\Phi_d \geq 1$, for all ω in Ω_N, then $\|\mathcal{T}\| \geq \|T_d\|_\infty$; i.e., the L_2-induced norm of the discretized system gives a lower bound for the L_2-induced norm of the sampled-data system, as should be expected. The following result formalizes this observation.

Corollary 5.2.7
Under the assumptions of Corollary 5.2.6,

$$\lim_{\Phi_d \to 1} \|\mathcal{T}\| = \|T_d\|_\infty \tag{5.25}$$

$$\lim_{\Phi_d \to 1} \|\mathcal{S}\| = \|S_d\|_\infty \tag{5.26}$$

Proof: Proof of (5.25) is immediate from (5.22). For (5.26) we have the following from (5.23):

$$\begin{aligned} \lim_{\Phi_d \to 1} \|\mathcal{S}\| &= \lim_{\Phi_d \to 1} \sup_{\omega \in \Omega_N} \frac{|S_d(e^{j\omega T})| + 1 + \|S_d(e^{j\omega T})| - 1|}{2} \\ &= \max\{\|S_d\|_\infty, 1\} \\ &= \|S_d\|_\infty . \end{aligned} \tag{5.27}$$

□

Hence, for example, if $\|\Phi_d\|_\infty$ is close to 1, then $\|\mathcal{T}\| \approx \|T_d\|_\infty$ and $\|\mathcal{S}\| \approx \|S_d\|_\infty$, and we should expect little intersample activity. ◇

Remark 5.2.3 (An Alignment Condition) Notice that Φ_d is independent of the controller, but depends on the prefilter, plant, and hold function. This suggests a possibly interesting way of looking at an optimization problem; i.e., selecting a suitable discrete complementary sensitivity function T_d, and then choosing the prefilter and hold to minimize Φ_d. In particular, when $\Phi_d = 1$ the matrix on the RHS of (5.17) becomes singular, since the vectors $\mathbf{f}$ and $\mathbf{g}$ "align". Therefore, minimization of the intersample behavior may be interpreted as an "alignment condition" between the hold, plant, and prefilter. This remains as a topic for future investigation. Further related comments may be found in Hagiwara and Araki [1995]. ◇

5.2.2 Numerical Implementation

The expressions for the frequency-gains and L_2-induced norms obtained in the last section can be readily numerically implemented by computing G_d and F_d from (5.10) and (5.11). These computations can be approached as "special discretizations" by considering relations similar to (2.8). In this way, the arguments of $\sup_{\omega \in \Omega_N}$ in (5.15) and (5.17) are expressed by two rational transfer functions in $z = e^{j\omega T}$ — the frequency-gains of the sampled-data sensitivity operators. The induced norms can then be computed by a straightforward search of maxima over the finite interval Ω_N[5].

[5]Similar formulas have been derived for the case of ZOH in Leung et al. [1991, Theorem 3].

Computation of $F_d(e^{j\omega T})$

We compute (5.11) from the discretization $F_d(z) = T\mathcal{Z}\{\mathcal{S}_T\{\mathcal{L}^{-1}\{F(s)\tilde{F}(s)\}\}\}$ (see Figure 5.2), where $\tilde{F}(s)$ denotes $F(-s)^T$. Since F is a strictly proper rational function, the sampling of the output of $F\tilde{F}$ is well-defined.

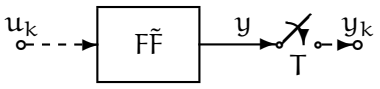

Figure 5.2: Scheme to compute $F_d(e^{j\omega T})$.

Let $\{a, b, c, 0\}$ be a minimal state-space realization of F. Then, a minimal realization for $F\tilde{F}$ is given by

$$A = \begin{bmatrix} a & bb^T \\ 0 & -a^T \end{bmatrix}, \quad B = \begin{bmatrix} 0 \\ -c^T \end{bmatrix}, \quad C = \begin{bmatrix} c & 0 \end{bmatrix} .$$

We then have the following.

Lemma 5.2.8 (Computation of $F_d(e^{j\omega T})$)
The function $F_d(e^{j\omega T})$ is given by

$$F_d(e^{j\omega T}) = TC(e^{j\omega T}I - e^{AT})^{-1}B.$$

Proof: At the sampling instants the state response of $F\tilde{F}$ is given by

$$\begin{aligned} x_{k+1} &= e^{AT}x_k + \int_0^T e^{A(T-\tau)}B\,u(\tau)d\tau \\ &= e^{AT}x_k + \int_0^T e^{A(T-\tau)}B\,\delta(\tau - T)\,d\tau u_k , \end{aligned} \tag{5.28}$$

where δ is Dirac's delta, since there is no hold device at the input of the system. From (5.28) we get the discrete system

$$\begin{aligned} x_{k+1} &= A_d x_k + B_d u_k \\ y_k &= Cx_k , \end{aligned}$$

where $A_d = e^{AT}$ and $B_d = B$. The result then follows from application of Lemma 2.1.2. □

Computation of $G_d(e^{j\omega T})$

The case of G_d is slightly more complicated than the previous one, but can be approached in a similar fashion. From (5.10) we have

$$\begin{aligned} G_d(e^{j\omega T}) &= \sum_{k=-\infty}^{\infty} G_k^*(j\omega)G_k(j\omega) \\ &= \frac{1}{T}C_d^*(e^{j\omega T})S_d^*(e^{j\omega T})E_d(e^{j\omega T})S_d(e^{j\omega T})C_d(e^{j\omega T}), \end{aligned}$$

where

$$E_d(e^{j\omega T}) \triangleq \frac{1}{T}\sum_{k=-\infty}^{\infty} H_k^*(j\omega)P_k^*(j\omega)P_k(j\omega)H_k(j\omega). \tag{5.29}$$

Hence, to compute G_d we need to evaluate $E_d(e^{j\omega T})$. We do this by discretizing the system depicted in Figure 5.3, i.e., the cascade of the hold $\tilde{H}$, the system $P\tilde{P}$, and the hold H. Since H is proper by definition, so is the cascade, and therefore the sampling operation is again well-defined.

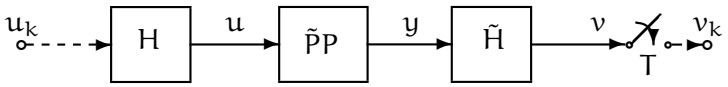

Figure 5.3: Scheme for computing (5.29).

Suppose that the plant P has a minimal realization $\{a, b, c, d\}$. Then, a minimal realization for $\tilde{P}P$ is given by

$$A = \begin{bmatrix} a & 0 \\ c^T c & -a^T \end{bmatrix}, \quad B = \begin{bmatrix} b \\ c^T d \end{bmatrix}, \quad C = \begin{bmatrix} d^T c & -b^T \end{bmatrix}, \quad D = \begin{bmatrix} d^T d \end{bmatrix}$$

We consider the case of a FDLTI GSHF; similar derivations are also valid for a PC GSHF. As seen in Chapter 3, a LTI GSHF is defined by a pulse response h,

$$h(t) = \begin{cases} Ke^{L(T-t)}M & \text{if } t \in [0, T) \\ 0 & \text{otherwise} \end{cases}, \tag{5.30}$$

for matrices K, L, and M of appropriate dimensions. The following lemma gives a formula for the computation of $E_d(e^{j\omega T})$ given the matrices A, B, C, D, and K, L, M.

Lemma 5.2.9 (Computation of $E_d(e^{j\omega T})$)
The function $E_d(e^{j\omega T})$ in (5.29) *is given by*

$$E_d(e^{j\omega T}) = C_d(e^{j\omega T}I - A_d)B_d + D_d, \tag{5.31}$$

where

$$A_d = e^{AT}$$

$$B_d = \int_0^T e^{A\tau}BKe^{L\tau}M\,d\tau$$

$$C_d = \int_0^T M^T e^{L^T(T-\tau)}K^T Ce^{A\tau}\,d\tau$$

$$D_d = \int_0^T M^T e^{L^T\tau}K^T DKe^{L\tau}M\,d\tau + \int_0^T M^T e^{L^T(T-\tau)}K^T C\int_0^\tau e^{A(\tau-\sigma)}BKe^{L(T-\sigma)}M\,d\sigma d\tau$$

Proof: We discretize the system of Figure 5.3 in four steps. Suppose t is in the interval $[kT,(k+1)T]$. First we compute the continuous-time response of the hold H to a pulse in u_k. This is

$$u(t) = Ke^{L((k+1)T-t)}Mu_k. \tag{5.32}$$

Second, feed u from (5.32) into $P\tilde{P}$ to get

$$\begin{aligned} x(t) &= e^{A(t-kT)}x_k + \int_0^{t-kT} e^{A(t-kT-\sigma)}BKe^{L(T-\sigma)}Md\sigma\, u_k \qquad (5.33)\\ y(t) &= Cx(t) + DKe^{L((k+1)T-t)}M\, u_k. \qquad (5.34) \end{aligned}$$

Third, compute the response of the hold $\tilde{H}$ to the output y given by (5.34) above. By Lemma 3.1.5 we know that the frequency response of the LTI GSHF is $H(s) = K(sI+L)^{-1}(e^{LT}-e^{-sT})M$. Let $\tilde{h}$ denote the impulse response of the "conjugated" hold whose frequency response is $\tilde{H}(s) = M^T(sI-L^T)^{-1}(e^{-L^TT}-e^{-sT})e^{L^TT}e^{sT}K^T$. Here, we neglect for the moment the "advance" of one sampling period due to the non-causality of $\tilde{H}$, i.e., we are considering $e^{-sT}\tilde{H}(s)$ instead. It follows then that

$$\tilde{h}(t) = \begin{cases} M^Te^{L^Tt}K^T & \text{if } t\in[0,T) \\ 0 & \text{otherwise} \end{cases}. \tag{5.35}$$

We get

$$\begin{aligned} v(t) &= \int_{kT}^{t} \tilde{h}(t-\tau)\, y(\tau)\, d\tau \\ &= \int_0^{t-kT} M^Te^{L^T(t-kT-\tau)}K^TC\, x(\tau+kT)\, d\tau \\ &\quad + \int_0^{t-kT} Ke^{L^T(t-kT-\tau)}K^TD\, u(\tau+kT)\, d\tau. \end{aligned} \tag{5.36}$$

Denote the first integral on the RHS of (5.36) by v_1, and the second by v_2. Replace $x(\tau+kT)$ and $u(\tau+kT)$ in (5.36) using (5.33) and (5.32) to obtain

$$\begin{aligned} v_1(t) = &\left(\int_0^{t-kT} M^Te^{L^T(t-kT-\tau)}K^TCe^{A\tau}\, d\tau\right) x_k \\ &+ \left(\int_0^{t-kT} M^Te^{L^T(t-kT-\tau)}K^TC\int_0^{\tau} e^{A(\tau-\sigma)}BKe^{L(\tau-\sigma)}M\, d\sigma d\tau\right) u_k, \end{aligned} \tag{5.37}$$

and

$$v_2(t) = \left(\int_0^{t-kT} M^Te^{L^T(t-kT-\tau)}K^TDKe^{L(T-\tau)}M\, d\tau\right) u_k. \tag{5.38}$$

Finally, we evaluate $v = v_1 + v_2$ at $t = (k+1)T$, which renders

$$\begin{aligned} x_{k+1} &= A_dx_k + B_du_k \\ v_{k+1} &= C_dx_k + D_du_k, \end{aligned} \tag{5.39}$$

where A_d, B_d, C_d and D_d are as claimed. To conclude, compute the $\mathcal{Z}$-transform of the expressions in (5.39) above, and eliminate X to get

$$zV(z) = (C_d(zI - A_d)^{-1}B_d + D_d)U(z). \tag{5.40}$$

If we introduce now the advance of one sampling period neglected before, the factor z on the RHS of (5.40) is canceled, rendering $E_d(z) = V(z)/U(z) = C_d(zI - A_d)^{-1}B_d + D_d$. Application of Lemma 2.1.2 gives the result. □

Remark 5.2.4 Matrices B_d, C_d and D_d in the above expressions can be easily numerically evaluated using matrix exponential formulas suggested by Van Loan [1978]. So, we have

$$\begin{aligned}
B_d &= [e^{AT} \quad 0] \exp\left\{\begin{bmatrix} -A & BK \\ 0 & L \end{bmatrix} T\right\} \begin{bmatrix} 0 \\ M \end{bmatrix}, \\
C_d &= [M^T \quad 0] \exp\left\{\begin{bmatrix} L^T & K^T C \\ 0 & A \end{bmatrix} T\right\} \begin{bmatrix} 0 \\ I \end{bmatrix}, \\
D_d &= [M^T e^{LT} \quad 0] \exp\left\{\begin{bmatrix} -L^T & K^T DK \\ 0 & L \end{bmatrix} T\right\} \begin{bmatrix} 0 \\ M \end{bmatrix} \\
&\quad + [M^T \quad 0] \exp\left\{\begin{bmatrix} L^T & K^T C & 0 \\ 0 & A & BK \\ 0 & 0 & -L \end{bmatrix} T\right\} \begin{bmatrix} 0 \\ e^{LT} M \end{bmatrix}.
\end{aligned}$$

◇

Example 5.2.1 (Sensitivity of gain-margin improvement with GSHFs) The use of these formulas is illustrated by computing the "frequency gain" of a system from an example in Yang and Kabamba [1994]. In this paper the authors present a technique based on GSHFs to achieve arbitrary gain-margin improvement of a feedback system.

The plant considered in the example is the following,

$$P(s) = \frac{s-2}{(s-1)(s+2)}.$$

Since the plant is non-minimum phase, there is a limit to the gain-margin achievable by LTI compensation Khargonekar et al. [1985], which in this case is 4.

Using the technique suggested by Yang and Kabamba, this plant can be stabilized by a FDLTI GSHF (Definition 3.1.1) determined by the matrices

$$K = \begin{bmatrix} 0 & 1 \end{bmatrix}, \quad L = \begin{bmatrix} 0 & 2 \\ 1 & -1 \end{bmatrix}, \quad M = \begin{bmatrix} -12616 \\ 312.8194 \end{bmatrix},$$

and a sampling period of $T = 0.05$, yielding a gain-margin of 10. However, this improvement of gain-margin comes at the cost of a very large sensitivity to input disturbances. Indeed, consider the feedback loop of Figure 5.4, where we have introduced a plant input disturbance c. Figure 5.5 shows the frequency-gain of

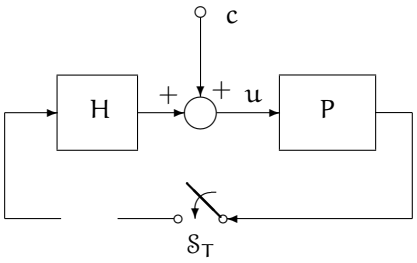

Figure 5.4: System with plant input disturbance.

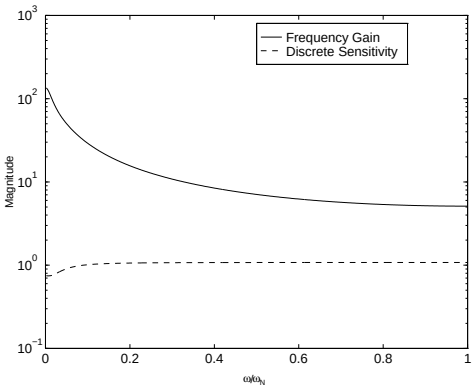

Figure 5.5: Hybrid frequency gains.

the hybrid operator on L_2 mapping c to u. For comparison we also plotted the frequency response of the discrete sensitivity function S_d.

The corresponding L_2-induced norms are

$$\begin{aligned} \|\mathcal{S}\| &= 134.69 \\ \|S_d\|_\infty &= 1.0785, \end{aligned}$$

which display a great difference. In a sense, this says that the discretized model does not represent the true behavior of the system. Indeed, these norms show that taking in account just the sampled behavior in this system gives only a very conservative lower bound of the actual L_2-gain of the hybrid system. As a consequence, a significant part of the system's dynamics is "hidden" from a sampled analysis as intersample activity. A large $\|\mathcal{S}\|$ means high sensitivity to L_2 plant input disturbances, which is particularly problematic if in addition there exist plant input saturations. Furthermore, a large $\|\mathcal{S}\|$ will also imply poor robustness properties to time-varying perturbations Sivashankar and Khargonekar [1993]. ◇

5.3 Summary

This chapter has considered the hybrid sensitivity and complementary sensitivity operators on L_2. We have described a mathematical framework called "frequency-domain lifting", which provides a representation of these operators as infinite dimensional "transfer matrices". Based on this representation we have characterized the frequency-gains of these operators as the maximum eigenvalue of an associated finite dimensional discrete transfer matrix. The L_2-induced norm of the operators is then computed by performing a search of maxima of these eigenvalues over a finite interval of frequencies. The expressions obtained can be easily implemented numerically to any desired degree of accuracy in a reliable fashion.

Similar expressions have been communicated in the literature for the case of the compact operators, like the complementary sensitivity operator [e.g., Hagiwara and Araki, 1995]. Hybrid non-compact operators impose additional difficulties in the evaluation of frequency-gains and L_2-induced norms Yamamoto and Khargonekar [1993]. Perhaps most interesting in our results is the fact that also the sensitivity operator, which is non-compact, can be characterized as a finite dimensional eigenvalue problem feasible of a numerically reliable implementation.

These formulas have immediate application in the analysis of stability robustness for LTV unstructured perturbations, and H_∞ control synthesis problems. Particularly, since our expressions allow the use of GSHFs, they provide a reliable computational tool for the evaluation of performance of a general class of sampled-data designs.